

Comparative study of plasma-deposited fluorocarbon coatings on different substrates

This article has been downloaded from IOPscience. Please scroll down to see the full text article.

2011 J. Phys. D: Appl. Phys. 44 194007

(<http://iopscience.iop.org/0022-3727/44/19/194007>)

View [the table of contents for this issue](#), or go to the [journal homepage](#) for more

Download details:

IP Address: 150.140.192.152

The article was downloaded on 14/06/2011 at 16:02

Please note that [terms and conditions apply](#).

Comparative study of plasma-deposited fluorocarbon coatings on different substrates

E Farsari, M Kostopoulou, E Amanatides, D Mataras and D E Rapakoulias

Plasma Technology Laboratory, Department of Chemical Engineering, University of Patras, PO Box 1497, 26504 Patras, Greece

E-mail: dim@plasmatech.gr

Received 30 September 2010, in final form 10 December 2010

Published 27 April 2011

Online at stacks.iop.org/JPhysD/44/194007

Abstract

The deposition of hydrophobic fluorocarbon coatings from C_2F_6 and $C_2F_6-H_2$ rf discharges on different substrates was examined. Polyester textile, glass and two different ceramic compounds were used as substrates. The effect of the total gas pressure, the rf power dissipation and the deposition time on the hydrophobic character of the samples was investigated. Films deposited on polyester textiles at low pressure (0.03 mbar) and power consumption (16 mW cm^{-2}) using pure C_2F_6 presented the highest water contact angles ($\sim 150^\circ$). On the other hand, the addition of hydrogen was necessary in order to deposit stable hydrophobic coatings on glass and ceramic substrates. Coatings deposited on glass at intermediate deposition rates ($\sim 100 \text{ \AA min}^{-1}$) and pressures presented the highest angles ($\sim 105^\circ$). Concerning the heavy clay ceramics, samples treated in low-pressure (0.05 mbar) and low-power (16 mW cm^{-2}) discharges showed the highest contact angles. The deposition time was found to play an important role in the hydrophobicity and long-term behaviour of porous and rough substrates.

1. Introduction

Recently, there has been a growing research and technological interest in the production of hydrophobic and self-cleaning surfaces [1]. Hydrophobic surfaces find applications in several industrial sectors such as in the textiles, automotive, glass, food packaging and building materials industries. Plasma polymerization of fluorinated organic compounds has been widely employed as a method to produce these hydrophobic and super-hydrophobic surfaces in a reliable, fast and cost-effective manner [2]. Nevertheless, the physical and chemical properties of plasma-deposited fluorocarbon coatings depend on various parameters such as the precursor gas, the substrate material and the plasma conditions.

The decomposition of fluorocarbon gases in electric discharges leads in a first step to the production of CF_x ($1 < x < 3$) fluorine atoms and ions which can either react in the gas phase or diffuse and can take part in the surface growth. CF_x radicals are the building blocks of the grown fluoropolymer film, their concentration in the gas phase

directly affecting the polymerization rate. On the other hand, fluorine atoms etch the surface and thus the total deposition rate is a result of these two competing processes [3]. d' Agostino *et al* [4, 5] proposed an ion-activated model to describe the deposition mechanism of fluorocarbon coatings. According to this model the deposition occurs on specific surface sites which are activated via ion bombardment. Moreover, O' Keefe and Rigsbee [6] have pointed out that, during the initial stages of the process, growth occurs in localized areas of the substrate thus allowing interaction between plasma and the uncovered substrate surface as well as with growing film areas. This situation alters the relative rates of deposition and etching on different substrates and in consequence can determine the F/C ratio and the CF_x distribution in the coating.

The deposition rate and the chemical composition of coatings deposited on a specific substrate are determined by the relative densities of CF_x radicals and fluorine in the discharge. These quantities depend on the precursor gas and the process conditions. When the F/C ratio of the fluorocarbon gas is high the F/ CF_x ratio in the discharge is also high

and the polymerization is inhibited. However, the monomer fragmentation can be reduced by adjusting input power and pressure thus enhancing the deposition rate [7–10].

A further increase in the deposition rate can be achieved by adding hydrogen in the gas feed [3, 11–14]. Hydrogen reacts with fluorine atoms producing HF which does not etch the material. Moreover, H abstracts F atoms from CF_x radicals (mainly from CF_3) towards species with a lower fluorination degree. Therefore, the fluorine content and consequently the composition of the coating can be controlled by the hydrogen content in the mixture. High hydrogen content leads to coatings with lower F/C ratio, higher cross linking and thus lower hydrophobicity.

The purpose of this work is to define optimum PECVD conditions for the deposition of stable hydrophobic coatings on different substrates such as polyester textiles, common glass as well as ceramic compounds typically used as building materials. Pure C_2F_6 and C_2F_6 in H_2 mixtures were used as film precursors. The effect of the gas feed composition, the total gas pressure, the real power dissipated in the plasma and the deposition time was investigated in order to obtain optimal hydrophobic properties of the coatings on these very different substrates. The variation of the deposition conditions and gas mixture required to optimize the process for each of the substrates are also discussed.

2. Experimental

The film depositions were carried out in a high-vacuum capacitively coupled parallel-plate reactor operating at a radio-frequency (rf) of 27.12 MHz (continuous wave) that has been described in detail elsewhere [15]. Briefly, the upper electrode (rf) is connected to the power generator (Dressler Cesar 276) via a pi-type automated matching network while the bottom grounded electrode works as the substrate holder.

The chamber pressure is controlled via a throttle valve controller, while the gas flow rates are independently adjusted using mass flow controllers. Pure hexafluoroethane (Linde, N3.5) or in mixtures with hydrogen (BOC, N6.0) were used as precursor gases.

Several plasma diagnostics were employed for investigating the process. More precisely, electrical (rf voltage and current) measurements were applied for the determination of the real power consumed in the discharge, the discharge current and impedance, using a reliable method as described in [16]. The deposition rate on glass substrates was measured *in situ* using laser reflectance interferometry.

The chemical composition of the deposited coatings was studied using x-ray photoelectron spectroscopy (XPS, SPECS LHS-10UHV), while the film morphology was monitored with scanning electron microscopy (SEM, JEOL 6300). The hydrophobic character of the coatings was evaluated by measuring the wetting angle of the sample in contact with water (WCA), while measurements of the rate of water droplet absorption were also performed (Krüss, DSA100S).

Polyester textile, common glass and clay ceramic compounds were used as substrates. Concerning the heavy clay ceramics two different compounds were used, a red one

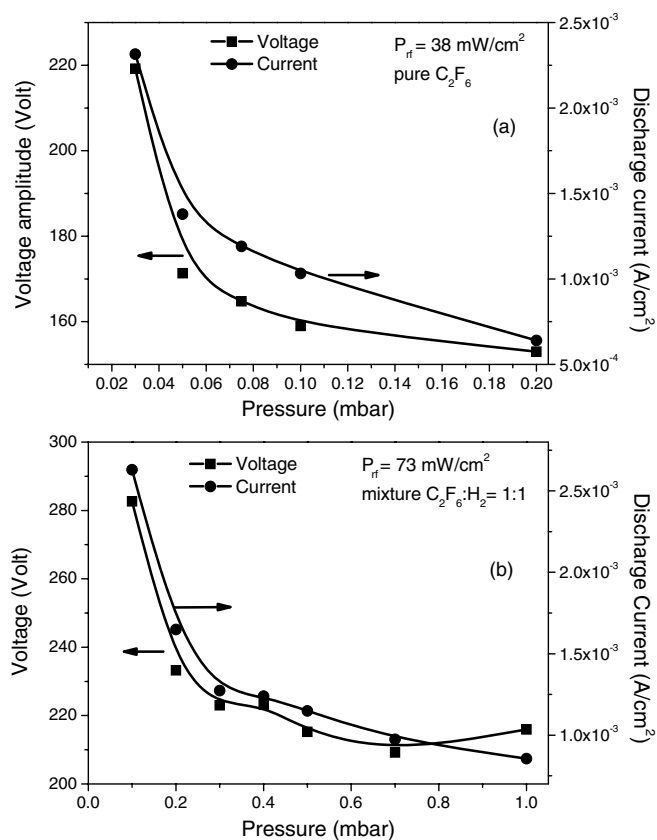


Figure 1. Amplitude of the applied rf voltage (left axis) and discharge current (right axis) as a function of the gas pressure for constant power dissipation: (a) pure C_2F_6 , $P = 38 \text{ mW cm}^{-2}$; (b) $C_2F_6-H_2$ mixture (50%), $P = 73 \text{ mW cm}^{-2}$.

(porosity: 25%, 72.6% SiO_2 , 10.33% CaO) and a white one (porosity: 35%, 46.9% SiO_2 , 12.33% CaO).

3. Results and discussion

The deposition of hydrophobic coatings on polyester textiles, glass and ceramic substrates from pure C_2F_6 and $C_2F_6-H_2$ rf discharges was investigated over a wide range of discharge powers and gas pressures. The effect of pressure was studied under constant power conditions and therefore a set of plasma electrical measurements was performed prior to the depositions to establish proper electrical conditions leading to constant power consumption as pressure is varied. Figure 1 presents the applied rf voltage (left axis) required to maintain constant power consumption as well as the discharge current (right axis) for pure C_2F_6 (figure 1(a)) and $C_2F_6-H_2$ 1:1 mixtures (figure 1(b)), as a function of the gas pressure. The increase in pressure imposes a drop in the applied voltage in order to maintain constant power consumption (38 mW cm^{-2} for pure C_2F_6 and 73 mW cm^{-2} for C_2F_6/H_2 mixture). This is mainly due to the enhancement of electron–molecule inelastic collisions with pressure. It is also worth noting that the values of the self-bias voltage are almost zero for all conditions presented here since the area of the powered electrode is almost equal to the sum of the areas of the substrate holder and the reactor walls. Moreover, the frequency of 27.12 MHz used

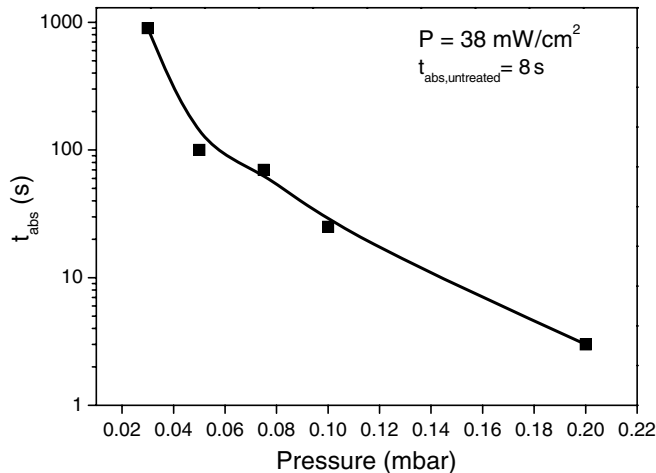


Figure 2. Absorption time of water droplets on the surface of treated textiles as a function of the gas pressure under conditions of constant power dissipation (38 mW cm^{-2}).

in this study favours electrical symmetry. The total discharge current drops with pressure either in the pure C_2F_6 discharges (figure 1(a)) or in the $\text{C}_2\text{F}_6\text{-H}_2$ 1 : 1 mixtures (figure 1(b)). The discharge current and, more precisely, the current flow in the bulk of the plasma present a linear relation to the electron drift velocity and the electron density [17]. The increase in pressure will result in an electron mobility drop and consequently in a drop in electron drift velocity. An estimation of the variation of electron density with pressure can be done using these electrical measurements and more precisely the discharge phase impedance and the resistive part of the total discharge impedance [18, 19]. Application of the analysis of [17, 19] to the present conditions showed that the average electron density clearly drops with pressure for pure C_2F_6 discharges from a value of $1.1 \times 10^{14} \text{ m}^{-3}$ at 0.03 mbar to $5.8 \times 10^{13} \text{ m}^{-3}$ at 0.2 mbar. On the other hand, for the mixtures of C_2F_6 in H_2 the situation is more complicated and the calculated electron density drops from a value of $2.5 \times 10^{14} \text{ m}^{-3}$ at 0.1 mbar to a minimum value of $1.8 \times 10^{14} \text{ m}^{-3}$ at 0.3 mbar. A further increase in pressure results in a continuous increase in electron density, which reaches a value of $2.4 \times 10^{14} \text{ m}^{-3}$ at 1 mbar. For the above-mentioned calculations of the average electron densities, an average electron temperature of 2 eV was considered, while the momentum transfer collision frequencies for C_2F_6 and H_2 were calculated from the corresponding cross sections [20, 21] and have values $4.1 \times 10^9 \text{ s}^{-1} \text{ mbar}^{-1}$ and $3.2 \times 10^9 \text{ s}^{-1} \text{ mbar}^{-1}$, respectively.

Under the conditions of figure 1(a) films were grown on polyester textiles, glass and ceramic compounds, with a 15 min processing time. The effect of pressure under constant power dissipation on the hydrophobic/hydrophilic character of the textile samples was determined by measuring the rate of water droplet absorption. Figure 2 presents the absorption time of water droplets ($V_{dr} = 0.5 \text{ ul}$) on the treated textiles as a function of the gas pressure. At the highest pressure (0.2 mbar) etching dominates over deposition as indicated by the absorption time (3 s) which is lower than that of the untreated textile (8 s). As pressure decreases, the deposition rate is gradually enhanced and at the lowest

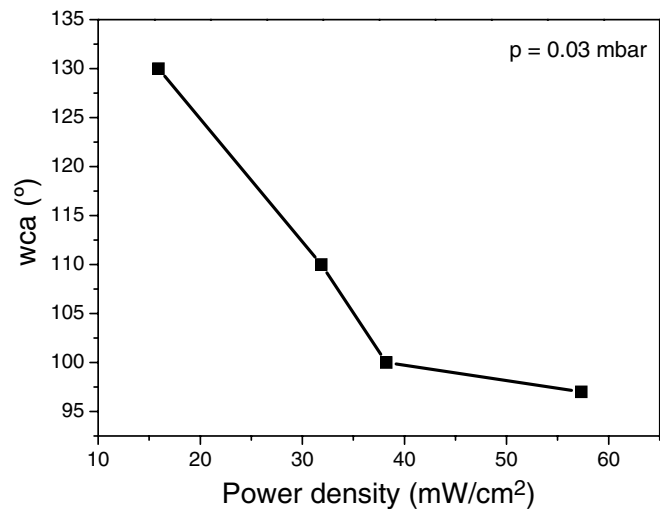


Figure 3. Wetting angles of textiles in contact with water as a function of the power dissipation at constant pressure (0.03 mbar).

Table 1. Water contact angles of treated textiles for different deposition times.

t_{dep} (min)	WCA ($^\circ$)
15	130
60	135
90	140
120	148
150	145

pressure (0.03 mbar) the droplets remain on the surface until they evaporate. As long as the deposition conditions are established the apparent water contact angle reaches values of $\sim 98^\circ$.

Furthermore, in order to increase the water contact angles on the treated surfaces a set of depositions was performed as a function of the discharge power, while maintaining the pressure at the previous optimal value (0.03 mbar) and the deposition time at 15 min. The apparent WCAs of coatings deposited on textiles as a function of power consumption are shown in figure 3. All the values are higher than 95° proving the hydrophobic character of coatings deposited in the range $16\text{--}57 \text{ mW cm}^{-2}$. The wetting angle reaches its highest value (130°) at the lowest power (16 mW cm^{-2}). Therefore, it appears that the lower the fragmentation of the fluorinated gas precursor, obtained by lowering both pressure and power, the higher the water contact angles of the treated textiles.

As a further step for optimization, the effect of the process time on the WCA values was investigated. Table 1 summarizes the results of this study showing that a maximum value of 148° was found for the sample treated for 120 min. In fact, as the process time and the film thickness increase, the fluoropolymer covers the fibres and the pores of the textile ($\sim 10 \mu\text{m}$ estimated from SEM images), as was also identified by XPS measurements. Figures 4(a) and (b) show the deconvolution of the XPS spectra of the C1s core for samples processed for 30 min and 120 min, respectively. The percentage of each of the functional groups is summarized in table 2. The surface content in -COOR groups (polyester

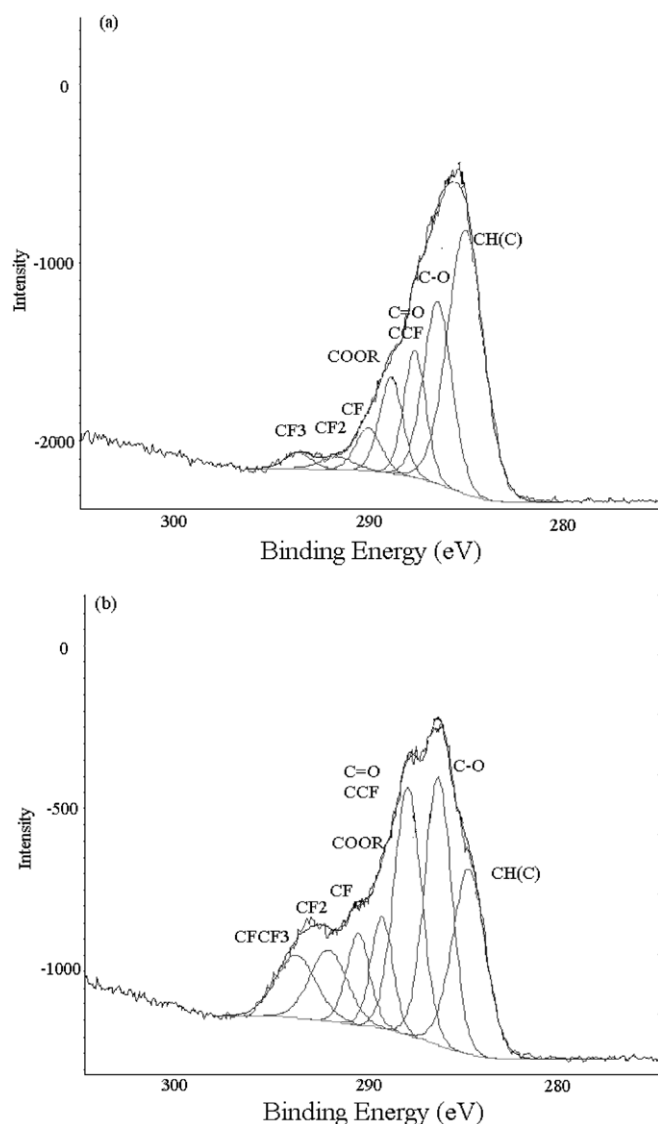


Figure 4. Deconvoluted XPS spectrum of the C1s core: (a) 30 min treatment and (b) 120 min treatment.

Table 2. % content of functional groups as a function of deposition time.

Deposition time (min)	Functional group %						
	CH(C)	C-O	C=O; CCF	COOR	CF	CF ₂	CFCF ₃
30	44	24	13	10	5	2	2
120	21	24	23	8	7	9	8

textile) decreases with processing time while the % content in $-CF_x$ groups increases. In addition, the fluorination degree is also enhanced (35% after 120 min) revealing that the coating density becomes higher, which in turn explains the higher WCA values.

Even though the deposition of stable hydrophobic coatings on polyester textiles using pure C_2F_6 was achieved, the results were not reproducible on glass and ceramic substrates. The glass and the ceramics coated under the same conditions with the textiles were either etched or the deposited hydrophobic coatings had bad adhesion with the substrates after contact with

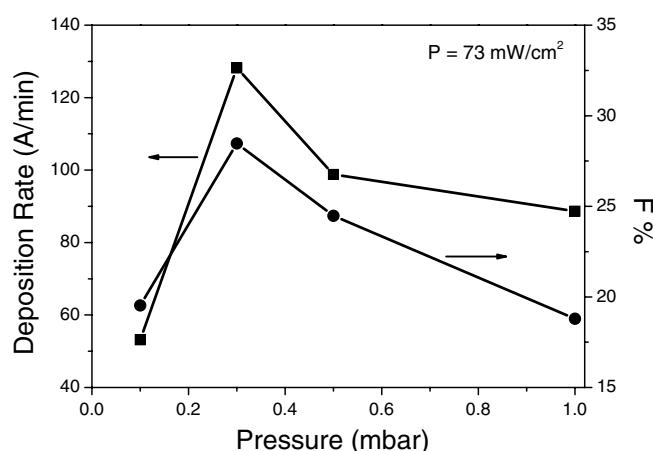


Figure 5. Deposition rate and %F content of the coatings as a function of the total gas pressure at constant power dissipation (73 mW cm^{-2}).

water droplets. Therefore, the addition of H_2 in the mixture of C_2F_6 was tested, in order to capture fluorine atoms and favour deposition [12].

Under the conditions of figure 1(b) (pressure range 0.1–1.0 mbar and power density 73 mW cm^{-2}) depositions were performed on glass and ceramics. Figure 5 presents the deposition rate (left axis) and the fluorine content of coatings deposited on the glass substrates (right axis). Both growth rate and fluorination degree present a maximum at 0.3 mbar. The maximum of the deposition rate may be again explained by the competitive processes of deposition from CF_x radicals and etching from F atoms according to the ion activation model [13]. For pressures below 0.3 mbar, the deposition rate drops (55 Å min^{-1}) due to the lower gas density and consequently to the lower rate of species production. On the other hand, the increase in pressure above 0.3 mbar causes also a decrease in the deposition rate. At higher pressures the ratio of F atoms relative to polymerization species (CF_x) seems to be favoured and according to the activation model [13] this will lead to a drop in the film growth rate.

The % fluorination of the surface (figure 5, right axis) as determined from XPS measurements presents also a maximum at 0.3 mbar. For pressures below 0.3 mbar, the ratio of F atoms to CF_x precursors seems to be enhanced, according to the results of the deposition rate, as the consequent etching will reduce the fluorination degree. On the other hand, the increase in pressure will favour F abstraction by H atoms from CF_x radicals (mainly by CF_3) leading to less fluorinated film precursors [11–14]. Thus, the maximum in our case is reached under intermediate pressure conditions, where radicals with high fluorine content participate in the film growth.

Furthermore, the water contact angles of the treated glass and ceramics were measured and all films deposited under the above-mentioned conditions were hydrophobic as the values of the WCA were greater than 98° . The WCA values reached a maximum of 105° for the glass substrate and $119^\circ \pm 3^\circ$ for the red ceramic and these maxima were achieved at 0.5 mbar for both substrates. The roughness of the treated ceramic is in the micrometre range ($rms \sim 1 \mu\text{m}$) and enhances the apparent WCA value, compared with treated

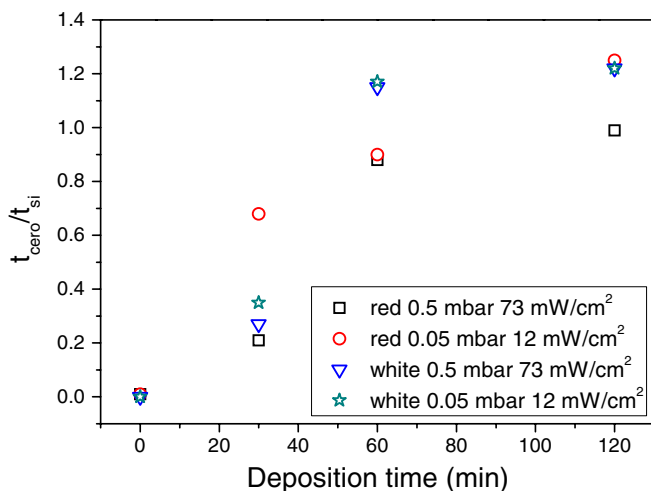


Figure 6. Residence time of water droplets on the treated surfaces divided by the corresponding times on a silicon wafer.

(This figure is in colour only in the electronic version)

glass (rms ~ 3 nm) [22, 23]. It should be noted that the WCA maximum values do not coincide with the maximum deposition rate (figure 5, left axis) or the fluorination degree (figure 5, right axis). Nevertheless, XPS analysis revealed that the peak at 292 eV, corresponding to CF_2 groups, is more intense for the samples deposited at 0.5 mbar. It should be mentioned that F/C ratio of the samples varied between 0.3 and 0.6, which is much smaller than the corresponding ratio of crystalline Teflon (F/C = 2) or typical Teflon-like films. The presence of hydrogen in the gas feed (50%) leads to lower F/C content in the coating and also to lower wetting angles.

In order to further optimize the deposition process of stable coatings on ceramic substrates the effect of the deposition time (30, 60, 120 and 240 min) on the hydrophobicity of the treated samples was studied. The experiments were carried out for two total gas pressures (0.05 and 0.5 mbar) and two discharge rf power consumptions (16 and 73 mW cm^{-2}), while the $\text{C}_2\text{F}_6 : \text{H}_2$ ratio was again 1 : 1. The morphological properties of the coatings were observed by SEM, while the hydrophobic character was also determined by measuring the apparent water contact angles and the absorption time of water droplets on the surface.

Figure 6 presents the residence time of water droplets on treated ceramics divided by the corresponding time on a silicon wafer (which does not absorb water) as a function of the deposition time. For a deposition time of 30 min, the surface coverage is not uniform due to the complex shape of the samples and it is possible that parts of the surface remain hydrophilic. Nevertheless, the rate of absorption was smaller than that of the untreated surfaces. The increase in the deposition time causes a further decrease in the absorption rate and after 60 min the droplets remain on the surface until they evaporate. At higher processing times the thickness of the fluorocarbon coating increases and gradually covers the pores of the substrate thus enhancing the hydrophobicity of the surface. Additional heating of the substrate from the plasma due to the rather long time of the process may also affect the film structure and density. This is better illustrated in figure 7,

where SEM images of the untreated ceramic (figure 7(a)) and coatings after 30 min (figure 7(b)), 60 min (figure 7(c)) and 240 min (figure 7(d)) are shown.

For a deposition time of 120 min, the apparent WCA reaches values of $119^\circ \pm 3^\circ$ and $110^\circ \pm 4^\circ$ for the red and the white sample, respectively, under the higher power consumption (73 mW cm^{-2}). The highest porosity of the white ceramic possibly explains the difference in the WCA values. Although there was no significant difference in the WCA of the red ceramic, the decrease in pressure (0.05 mbar) and power (16 mW cm^{-2}) caused an enhancement of WCA of the white compound which reached a value of $120^\circ \pm 3^\circ$. This is probably related to the increase in the deposition rate due to the lower fluorine production.

The deposition time also affects the long-term behaviour of the coatings. Water contact angles and water absorption rate measurements were performed for a period of 4 months after the deposition. All coatings deposited either at 0.5 mbar and 73 mW cm^{-2} or at 0.05 mbar and 16 mW cm^{-2} remained hydrophobic. Coatings deposited at the lower power and pressure did not present any ageing effects as the wetting angles were measured at $120^\circ \pm 3^\circ$. On the other hand coatings deposited on red substrates at 0.5 mbar and 73 mW cm^{-2} presented slightly smaller WCA values ($116^\circ \pm 3^\circ$). In both cases, the residence time of water droplets on the surface was even in that case high enough (>15 min), indicating that the surfaces remained hydrophobic.

4. Conclusions

The deposition of fluorocarbon coatings on different substrates was examined and the optimum conditions which lead to hydrophobic coatings were determined for each type of substrate. The growth of hydrophobic coatings on textiles was achieved using pure C_2F_6 as precursor gas, whereas the addition of hydrogen was necessary in order to improve the adhesion of the coatings on ceramic or glass substrates. In both cases, the effect of gas pressure, power consumption and deposition time was investigated.

Concerning the textile substrates, the coatings deposited at the lowest gas pressure (0.05 mbar) and power (16 mW cm^{-2}) presented the highest wetting angles in contact with water, which reached a value of 148° . By decreasing the gas pressure the density of F atoms was limited and thus the competitive etching process was suppressed. The lower power consumption led to higher WCA values due to the decrease in the density ratio between F atoms and CF_x radicals.

The total gas pressure and power consumption showed a similar effect when hydrogen was added to the gas feed. When the total gas pressure increases, the deposition rate presents a maximum of 128 \AA min^{-1} at 0.3 mbar, as a result of the competitive effect between etching and deposition. However, the higher fluorination degree, gained at the higher deposition rate, did not coincide with optimum hydrophobic properties of the coatings. Films deposited on glass substrates at higher pressure (0.5 mbar) showed higher WCA values (105°) mainly due to the way F atoms were bonded in the film. The corresponding values for the white and red ceramics were

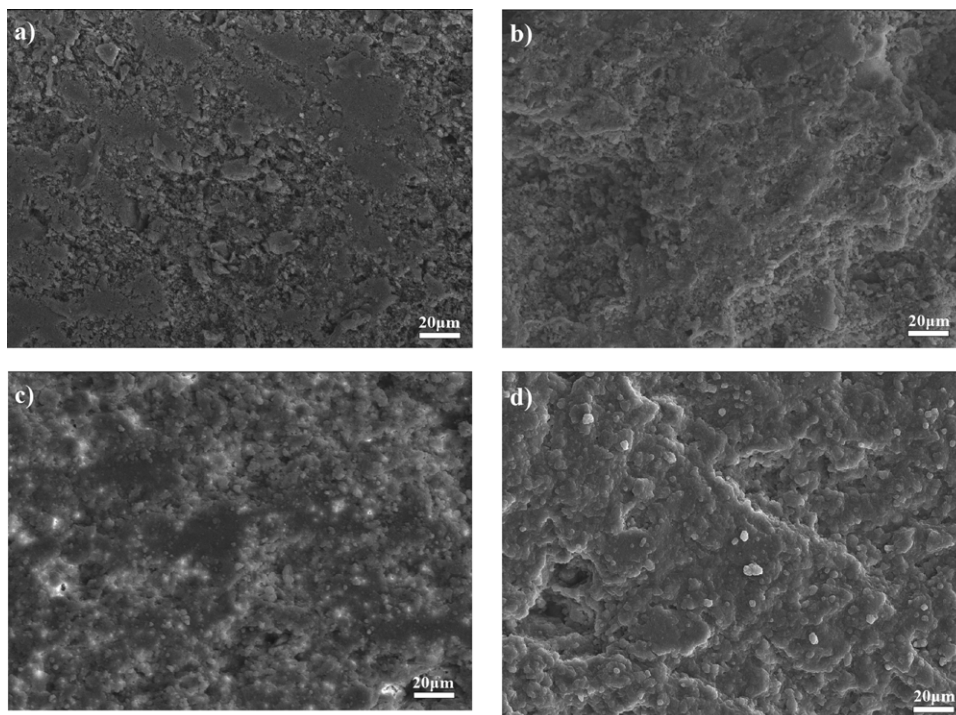


Figure 7. SEM images of coated ceramics for different deposition times: (a) untreated, (b) 30 min, (c) 60 min and (d) 240 min.

measured to be 110° and 119° , respectively, as the extremely rough surface of the ceramics enhanced hydrophobicity. The hydrophobicity of the white ceramics was further improved when pressure and power decreased further (0.05 mbar, 5 W).

Finally, the deposition of hydrophobic coatings on textiles and ceramics was strongly affected by their surface morphology. Because of the high porosity, high deposition times (120 min) were needed to achieve high wetting angles. In almost all cases the hydrophobic properties remained extremely stable over a long period of time.

Acknowledgments

The authors wish to thank Dipartimento di Chimica and CNR-Istituto di Metodologie Inorganiche e dei Plasma (IMIP) at the University of Bari, Italy, and particularly Dr E Sardella for the XPS measurements and for the discussion of the results.

References

- [1] Dodiuk H, Rios P F, Dotan A and Kenig S 2007 *Polym. Adv. Technol.* **18** 746
- [2] Yasuda H K 1985 *Plasma Polymerization* (New York: Academic)
- [3] d' Agostino R, Cramarossa F and De Benedictis S 1982 *Plasma Chem. Plasma Process.* **2** 213
- [4] d' Agostino R, Cramarossa F, Fracassi F, Desimoni E, Sabbatini L, Zamboni P and Caporiccio G 1986 *Thin Solid Films* **143** 163
- [5] d' Agostino R, Cramarossa F and Illuzzi F 1987 *J. Appl. Phys.* **61** 2754
- [6] O' Keefe M J and Rigsbee J M 1994 *J. Appl. Polym. Sci.* **53** 1631
- [7] Iriyama Y and Yasuda H 1992 *J. Polym. Sci. A* **30** 1731
- [8] Favia P, Creatore M, Palumbo F, Colaprico V and d' Agostino R 2001 *Surf. Coat. Technol.* **142–144** 1
- [9] Mounstier T W and Samuels J A 1998 *Thin Solid Films* **332** 362
- [10] Loh I H, Klausner M, Baddour R F and Cohen R E 1987 *Polym. Eng. Sci.* **27** 861
- [11] Masuoka T and Yasuda H 1982 *J. Polym. Sci.* **20** 2633
- [12] Lamendola R, Favia P and d' Agostino R 1992 *Plasma Sources Sci. Technol.* **1** 256
- [13] Balazs D, Hollenstein C and Mathieu H J 2005 *Plasma Process. Polym.* **2** 104
- [14] d' Agostino R, Favia P, Fracassi F and Illuzzi F 1990 *J. Polym. Sci. A* **28** 3387
- [15] Voulgaris C, Panou A, Amanatides E and Mataras D 2005 *Surf. Coat. Technol.* **200** 351
- [16] Spiliopoulos N, Mataras D and Rapakoulas D 1996 *J. Vac. Sci. Technol. A* **14** 2757
- [17] Amanatides E and Mataras D 2001 *J. Appl. Phys.* **89** 1556
- [18] Godyak V A, Piejak R B and Alexandrovich B M 1991 *IEEE Trans. Plasma Sci.* **19** 660
- [19] Amanatides E, Hammad A, Katsia E and Mataras D 2005 *J. Appl. Phys.* **97** 073303
- [20] Pirgov P and Stefanov B 1990 *J. Phys. B: At. Mol. Opt. Phys.* **23** 2879
- [21] Frost L S and Phelps A V 1962 *Phys. Rev.* **127** 1621
- [22] Quere D 2002 *Physica A* **313** 32
- [23] Kulinich S A and Farzaneh M 2005 *Vacuum* **79** 255